Fohlmeister, J., Lechleitner, F. A. (2019): STAlagmite dating by radiocarbon (star): A software tool for reliable and fast age depth modelling. - *Quaternary Geochronology*, *51*, pp. 120—129.

DOI: http://doi.org/10.1016/j.quageo.2019.02.008

STAlagmite dating by Radiocarbon (star): a software tool for reliable and fast age depth modelling

Jens Fohlmeister[1,2], Franziska A. Lechleitner[3]

1 Institute of Earth and Environmental Science, University of Potsdam, Karl-Liebknecht-Straße 24, D-14476 Potsdam, Germany

2 GFZ German Research Centre for Geosciences, Section 5.2 Climate Dynamics and Landscape Development, Telegrafenberg, D-14473 Potsdam, Germany

3 Department of Earth Sciences, University of Oxford, South Parks Road, Oxford OX1 3AN, UK

Abstract

Speleothems, secondary cave carbonates, are important tools for climate reconstruction, especially as they often can be very precisely dated with the U-Th method. If the U-Th method fails, dating becomes difficult, and often results in abandonment of samples and study sites. Radiocarbon dating is the only other radiometric dating technique applicable to the last ~50 ka, but presents complexities related to temporal variability of the reservoir effect in speleothems. Thus, radiocarbon dating of speleothems is not straightforward, and there are currently no publicly available tools to define proper age-depth relationships with this method.

Here, we present an improved version of a previously published radiocarbon based age-depth modelling approach (*star*, Lechleitner et al., 2016b), which is now made freely available. The software is easy to use and provides the possibility to obtain reliable age-depth relationships, without prior knowledge of reservoir effects and their variability. In addition, *star* is able to detect and handle growth stops and phases with different growth rates. We test *star* on artificially constructed data sets and illustrate steps to improve the model performance. Furthermore, we apply the new approach to published radiocarbon data of U-Th dated stalagmites. This offers the possibility to investigate the strengths and weaknesses of the new approach with respect to potentially significant long term trends in the radiocarbon reservoir effect, which might otherwise remain undetected. In summary, we have produced a valuable software, which easily enables to construct age-depth relationships on the basis of reservoir effect disturbed radiocarbon measurements.

1. Introduction

Stalagmites are well established archives for climate reconstruction of the Late Quaternary (e.g., Fairchild and Baker, 2012). They offer the possibility to construct continuous, high resolution records of environmental variability. In combination with precise U-Th dating, important questions about the timing of climate-related events can be adequately addressed and leads and lags in the climate system can be investigated.

However, if the U-Th clock fails, either due to low U concentrations, especially challenging for young samples where not enough time passed for ^{230}Th to build up, or due to a high detrital component embedded in the crystal lattice, stalagmites are stripped of their powerful strength. Apart from annual layer counting methods, applicable only on few specimens, the only alternative dating method is provided by radiocarbon. Moreover, the carbon isotope composition is believed not to be affected by diagenesis (Zhang et al., 2014), and thus radiocarbon dating can be a useful tool to date specimens where U-Th dating will fail due to open-system conditions related to diagenesis.

Radiocarbon dating of stalagmites and other secondary carbonates is complex and not straightforward, due to the *a priori* quantitatively unknown and temporally variable reservoir effect (dead carbon fraction, 'DCF'). The reservoir effect has been shown to vary on a wide range of time scales. On annual time scales variations of up to 10 percent modern carbon (pMC) in radiocarbon activity have been observed in cave drip water (Fohlmeister et al., 2010; Minami et al., 2015). Decadal to centennial scale variations have been reported to range around 10 pMC (Griffiths et al., 2012, Lechleitner et al., 2016) and on millennial time scales variations can be larger than 15 pMC (Oster et al., 2010; Noronha et al., 2014), with extreme values higher than 20 pMC observed (Bajo et al., 2017). Different carbon (C) sources and their relative contribution to stalagmite $CaCO_3$ are responsible for these variations. The radiocarbon depleted host rock can introduce a reservoir effect of up to one radiocarbon half-life, but can also be negligible, depending on the conditions of carbonate dissolution. In addition, aged organic matter, either of the soil or from deep sources within the epikarst (e.g., Benavente et al., 2010; Noronha et al., 2015; Bergel et al., 2017) contributes to the reservoir effect. Variations in the reservoir effect are often related to changes in hydrology (Fohlmeister et al., 2010; Griffiths et al., 2012; Noronha et al., 2014; Lechleitner 2016; Bajo 2017) but can also be driven by aging or rejuvenation of organic matter sources or other, not yet understood processes (Oster et al., 2010; Rudzka et al., 2011).

First approaches to date stalagmites using radiocarbon corrected the measured radiocarbon age by an estimated and constant reservoir effect (e.g., Rudzka et al., 2012). A few years ago, Hua et al. (2012) proposed an interesting and powerful approach to date young speleothems. However, this method also still requires the assumption of a constant reservoir effect. Recently, Lechleitner et al. (2016b) developed a method with which radiocarbon dating of stalagmites is possible even without knowledge of the magnitude of the reservoir effect and without the need for the reservoir effect to remain constant in time. The only assumptions required in this approach are the stationarity of the reservoir effect (i.e., no long-term trends, but not necessarily constant) and no occurrence of major changes in the growth rate. This method has already been successfully applied to other stalagmite studies (Hua et al., 2017, Fohlmeister et al., 2017).

Here, we present an improved version of the approach published by Lechleitner et al. (2016b) now named *star*. Compared to the precursor work, the improved software version is now able to detect and handle growth stops as well as to find major changes in the growth rate. In addition, *star* advises the user about the credibility of the dating approach by evaluating trends in speleothem proxies – especially $\delta^{13}C$ and Mg/Ca, which often relate to variations in the reservoir effect.

2. Age modelling approach

The basic principles behind the age-modelling approach are well described in Lechleitner et al., (2016b). In short, *star* uses the radioactive decay of radiocarbon to evaluate how much time has passed since deposition of the speleothem $CaCO_3$. The common decay equation

$$A(t) = A(0)*\exp(-\lambda t), \qquad (1)$$

(with time, t, radiocarbon decay constant, λ, and the radiocarbon activity, A, where A(0) is not constant but a time-dependent function) can be translated to a depth scale, d, assuming a sufficiently constant growth rate, GR, by t = d/GR. Using the logarithm of equation (1) and replacing t by d and GR results in

$$\ln(A(t)/A(0)) = -d*\lambda/GR. \qquad (2)$$

A linear fit is applied to the natural logarithm of the radiocarbon values over stalagmite depth. The slope, s, of this fit equals λ/GR and thus provides a direct estimate of the mean growth rate of the stalagmite. Using a point of known age, i.e., an anchor point, it is possible to deduce a first-estimate age-depth relationship. The anchor point might be the stalagmite top in case of an active drip feeding the stalagmite, or it might be the onset of the nuclear bomb peak if this atmospheric radiocarbon anomaly is found in the stalagmite. If a high quality U-Th date is available, this point can also be used as an anchor point.

So far this approach assumes that the initial radiocarbon activity in the speleothem remained constant through time. Being well aware that this is unlikely due to the changes in the atmospheric radiocarbon concentration (Reimer et al., 2013), an iterative process that accounts for atmospheric radiocarbon variation is used. Starting with the age control from the first-estimate age-depth model, the atmospheric radiocarbon values (using IntCal13; Reimer et al., 2013) at the estimated time of carbonate deposition can be used to correct for the variability of the initial radiocarbon concentration (A0) in the stalagmite. With the corrected radiocarbon activities, the fitting procedure is repeated, resulting in a more accurate mean growth rate and an improved age-depth estimate than in the prior iteration. In turn, the new age-depth model of the second iteration provides the possibility to perform a better correction of the initial radiocarbon activity by atmospheric radiocarbon values, which can then be used to further improve the age-depth relationship. The process is iteratively repeated until convergence of the mean growth rate is obtained, e.g., when growth rate is not changing by more than 1/1000 in successive iteration steps.

So far, this section described the already available approach. In the next section, the three new modules will be explained and discussed.

2.1 First-order-check for stationarity of the radiocarbon reservoir effect

Please note that it is not necessary to have any prior knowledge about the magnitude of the reservoir effect to apply this method and that the method even allows for a variable reservoir effect. However, an important assumption for this method is the long-term stationarity of the reservoir effect (Lechleitner et al., 2016b), but this does not mean that the reservoir effect has to be constant through time. Cases where this assumption is violated will be discussed in sections 4.2 to 4.4.

The updated program version offers the possibility to evaluate the likelihood for the presence of long-term trends in the reservoir effect. This is done by analysing additional available stalagmite proxies, such as $\delta^{13}C$ and Mg/Ca. Both proxies are known to be related to reservoir effect variations (e.g., Griffiths et al., 2012; Noronha et al., 2014; Lechleitner et al., 2016). If long-term trends are present in one or both of the additional datasets the likelihood for a long-term trend in the reservoir effect is relatively high and *star* will pause and notify the user about a potential non-stationarity of the reservoir effect. It is possible to resume the age-depth modelling after the pause, but the final modelling results should be critically scrutinised by the user.

2.2 Detection and handling of growth stops

While outlier detection for radiocarbon measurements influenced by variations in the reservoir effect are not very meaningful and thus not implemented, potential growth stops can be detected with a new function. Significant and fast transitions from low to high ln(a14C) detected from old to young portions of the stalagmite are identified as potential growth stops. This method reliably detects growth stops for datasets with little variability in the reservoir effect, but is prone for false positive detections of growth stops if the reservoir effect is affected by large natural variability. It is therefore not possible to unequivocally define a growth stop, except with the help and experience of the user and taking into account other hints for growth stops, e.g., optically detectable layers in the stalagmite or anomalously large, rapid increases in Mg/Ca or $\delta^{13}C$. Therefore, *star* will only make suggestions on where growth stops might have occurred. The final decision has to be made by the user upon these suggestions.

After definition of the growth stop(s), the program checks which growth section the anchor point belongs to and starts with the age modelling of this section following the description in Sec. 2 (see also, Lechleitner et al., 2016b). For growth sections without an anchor point, the age-depth modelling procedure is slightly different. The average reservoir effect for the section with the anchor point is determined after modelling its age-depth relationship. With this average reservoir effect the radiocarbon measurements of the section(s) without an anchor point are corrected and calibrated. This ensemble of calibrated and reservoir effect corrected radiocarbon ages provides the most likely position of the mean growth rate determined by the slope of the depth vs ln(a14C(t)) relationship. All errors for the calibration and the reservoir correction are rigorously handled. This method is then repeated for all growth sections without anchor point determined by the user.

If an anchor point is available for each section bracketed by a growth stop, it is suggested to treat the sections as individual data sets. This is more precise as errors in sections without an anchor point are usually much larger due to the need for reservoir correction and calibration.

2.3 Detection and handling of growth rate changes

The most important improvement of the program is the newly implemented module for the detection and handling of growth rate changes within the speleothem. For purposes of a better illustration we produced an artificial radiocarbon data set for a 520 mm long stalagmite, with two major changes in growth rate (Fig. 1a). The growth rate was prescribed to be 0.221 mm/a between 581 mm and ~388 mm distance from top, 0.0554 mm/a between ~388 mm and 228 mm, and 0.1221 mm/a for the top part. Prescribing that the top of the stalagmite was actively growing at the time of collection, the age structure of this artificially constructed stalagmite is fixed, with growth starting ~5200 years before today. Along the length of the hypothetical stalagmite 31 radiocarbon measurements were equally but none-equidistantly distributed representing a possible straightforward sampling strategy for real stalagmites. For the construction of the radiocarbon data set we accounted for the radiocarbon concentration of the atmosphere and randomly added a reservoir effect of 15 +/- 3 % to the data, which represent varying effects from the dilution of the atmospheric signal through radiocarbon devoid host rock and pre-aged soil organic matter.

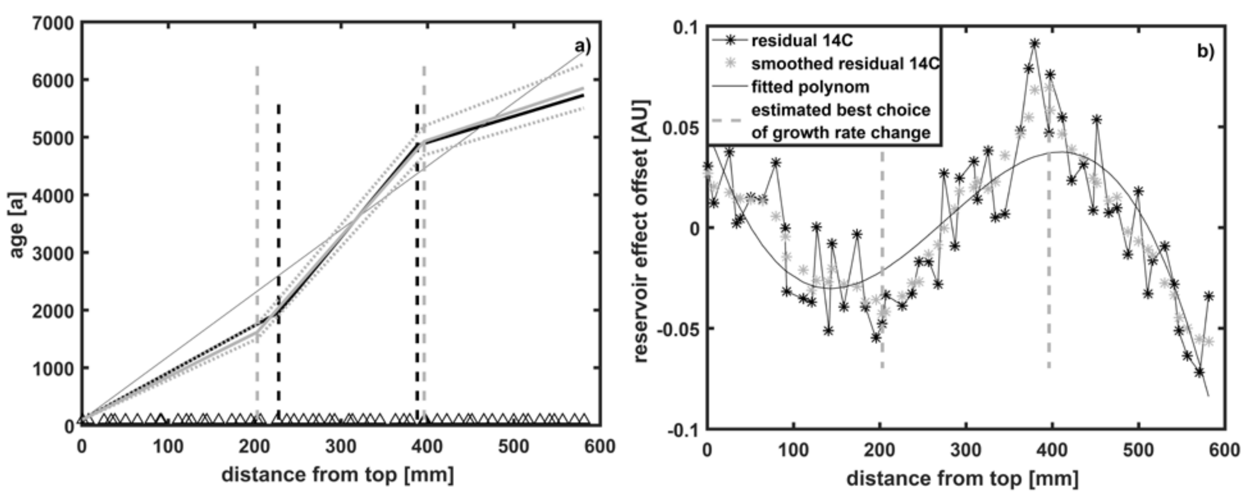

Figure 1: *Artificial radiocarbon data set for a 520 mm long hypothetical stalagmite, with two major changes in growth rate. a) Prescribed age-depth relationship in solid black, with position of radiocarbon data points (open triangles). Dashed black lines represent the prescribed location of growth rate changes. The modelled approximation of the age-depth relationship without taking into account growth rate changes is represented by the thin grey line. The final result after identifying the depths where growth rate changes occur is shown in thick grey, including error estimation (grey, dotted). Dashed grey lines represent the modelled positions of growth rate change. b) Offsets from the average reservoir effect (black stars) derived from the linear age-depth model are used to find the position of growth rate changes (dashed grey lines). They are defined by the extreme values of the smoothed offset from the average reservoir effect data series (grey stars). Solid thin polynomial reflects the best fit. The number of the extreme values of the best-fit polynomial determines the number of growth rate changes detected by the approach.*

We use this artificial radiocarbon dataset to deduce the prescribed age-depth relationship with our approach, trying to account for the changes in growth rate. First, the age-depth relationship is modelled as if the growth rate would have been constant throughout the stalagmite growth (Fig 1a). While this is an appropriate approximation of the truth, this result would lead to systematic shifts in the reservoir effect (Fig. 1b), which can be calculated from the first-guess linear age-depth model. At depths where the modelled linear approach is older (younger) than the true age-depth relationship, the reservoir effect appears smaller (larger) than the average. Assuming that these second-order offsets are uniquely induced by age-offsets, this systematic can be used to define the locations of the growth rate change. The program is taught to recognise such typical structures. A structure with one maximum and one minimum is indicative for two occasions where the growth rate changed: one around the position of the maximum offset and one at the minimum offset (Fig. 1b). The strategy for defining the position of the growth rate changes is to smooth the reservoir effect variations (offset from the average) with a five-point running mean and to determine the extreme points of this smoothed data set. After testing, we found that this approach reliably finds the best estimate for the position(s) of a growth rate change. Afterwards, *star* individually evaluates the growth rate for each section between the depths with growth rate changes (Fig. 1a), starting with the section with the anchor point and using the same algorithm as described in Sec. 2.

This method is best suited to detect growth rate changes for alternating growth rates, e.g., from slow to faster growth and back to a slower growth. However, gradual changes cannot be reliably detected, e.g., from fast to slow and even slower. In this scenario only one growth rate change is identified (fast to slow), in most cases close to the centre of the second growth rate section. This newly developed module allows to determine up to three positions of growth rate changes per growth section. Thus, for a stalagmite with one hiatus, up to six growth rate changes can be found and implemented in the age modelling procedure.

2.4 Running the program

The program is written and tested in Matlab (versions R2016a and R2016b). The model comes with a short, one-page manual, in which the user is led through a short 'getting started' section by running a specific artificial dataset (from Lechleitner et al., 2016b). To become familiar with the program it is also possible to run a randomly generated data set and a real data set (Fohlmeister et al., 2017).

Crucial information for running the *star* are the radiocarbon measurements, which need to be provided in fraction Modern (fM) including errors and sample depths. In addition, an anchor point including its age uncertainty is necessary. After the user's evaluation of possible suggested growth stops an age-depth relationship for the stalagmite is provided. This result comes without any discussion of its reliability. If $\delta^{13}C$ or Mg/Ca datasets (or both) were provided, *star* evaluates the reliability of the obtained age-depth relationship in terms of the state-of-the-art knowledge about the reservoir effect – proxy relationship (Griffiths et al., 2012, Noronha et al., 2014, Lechleitner et al., 2016b). As star is only evaluating long term trends for $\delta^{13}C$ or Mg/Ca, the proxy data does not need to be provided in high resolution. This is especially useful in case only a limited amount of data is measured, e.g., in order to provide them for star to check the obtained age-depth relationship.

The number of radiocarbon data points does not need to be high to obtain good results, but the results will be better constrained with a higher number of radiocarbon measurements. Especially if the user is expecting a major change in growth rate we recommend to measure at least ten radiocarbon samples to obtain a reliable result. Otherwise, it is prescribed to not test for changes, as our experience with this module showed that analysis of growth rate changes requires at least ten samples. Despite this, *star* can be run with only three available radiocarbon samples for simple age-depth models, but this is not advisable. The previous version of *star* was successfully used on a ~13cm long and 900 a old stalagmite with only six radiocarbon dates (Fohlmeister et al., 2017). In this example the radiocarbon reservoir effect was not varying strongly, and a reliable age model could be constructed with this approach. However, if the variation in the reservoir effect is large, it is advisable to measure a larger amount of samples. This reduces uncertainties in the fitting procedure and reduces the age error. The user can evaluate the extent of variation in the reservoir effect after obtaining the age-depth result for a first number of radiocarbon data points. If the age errors are large, then this is either due to a large variation in the reservoir effect or due a short growth period of the speleothem with respect to variations in the reservoir effect. *Star* can provide good results for stalagmites that grew over sufficiently long time periods (~> 2000 a), when the relative magnitude of variations in the reservoir effect becomes less important. For stalagmites with shorter growth periods (~< 1000 a) reservoir effect variations can significantly affect the reliability of the constructed age model.

3. Limits of the new functions

3.1 Stationarity of reservoir effects

As discussed in many studies investigating the influence of hydrology on the radiocarbon reservoir effect (DCF), there is a relationship between DCF and other hydrology related proxies such as Mg/Ca or $\delta^{13}C$ (Griffiths et al., 2012; Lechleitner et al., 2016a; Bajo et al., 2017). Usually this relationship is argued to be established by the negative correlation between the amount of precipitation and the Mg/Ca ratio caused by incongruent carbonate dissolution and prior calcite precipitation (e.g., Fairchild and Treble, 2009; Sinclair et al., 2012). The stable C isotope composition is influenced by variations in drip rate (infiltration of meteoric water and karst hydrology) through prior calcite precipitation and fractionation effects on the top of the stalagmite (e.g., Dreybrodt, 2008; Scholz et al., 2009; Dreybrodt and Scholz, 2011; Deininger et al., 2012; Fohlmeister et al., 2018). In contrast, the amount of precipitation is often correlated with the DCF as a result of variations of the carbonate dissolution conditions (Fohlmeister et al., 2010; 2011; Griffiths et al., 2012). Based on those assumptions, *star* checks for long-term trends in Mg/Ca and $\delta^{13}C$ to predict possible trends in the reservoir effect.

Studies where reservoir effect and Mg/Ca or $\delta^{13}C$ showed contemporeanous long-term trends are available (Scholz et al., 2012; Bajo et al, 2017) and support our method of DCF trend detection. However, the knowledge on C-transfer dynamics in karst systems is still limited (Lechleitner et al., 2016b) and the hydrology-based relationship between the reservoir effect and the other proxies might be violated if other processes counteract the known mechanisms. Therefore, predicting trends in the reservoir effect with the use of ancillary proxies should still be treated with great care, and the results should in any case be evaluated by the user. Future improvements in the understanding of C-transfer dynamics from the soil to the cave system will allow for a more reliable prediction of reservoir effect trends.

3.2 Detection of growth rate changes

We produced three sets of 20000 synthetic age-depth models each to analyse how variations in the reservoir effect, growth rate, and the number of radiocarbon measurements affect the detection and position of growth rate changes, as well as the precision of the modelled age-depth relationships. The three sets differ in their prescribed growth rate ranges (10 to 100 µm/a and 50 to 500 µm/a) and in the DCF variability (between 12 to 17% and between 6 and 23 %; Tab. 1). The artificially constructed growth history and accordingly prescribed synthetic radiocarbon data were produced completely randomly (uniform distribution) but within given constraints. Each synthetic stalagmite was prescribed to be between 10 and 20 cm long and had between 10 and 40 radiocarbon measurements, which were evenly but not equidistantly distributed across the length of the synthetic dataset. The depth of the growth rate change was randomly prescribed to be somewhere within the second third of the stalagmite. The growth rates of the two sections were determined randomly and independently from each other; i.e., the growth rate differences can be large or small. Each stalagmite stopped growing recently, i.e., the anchor point for all realizations is present-day at the stalagmite top.

Tab. 1: *Parameters and prescribed ranges for each of the three experiments. The 'normal' experiment accounts for small variations in growth rate and DCF, while the 'high DCF' experiment has a large variation in the reservoir effect and the 'fast growth' experiment is designed to investigate our model approach under faster growth rates. For each experiment 20000 artificial data were generated.*

Experi-ment	Length range [cm]	Number of 14C points	Location of growth rate change	Growth rate range [µm/a]	DCF variability [%]	Growth rate change detected [%]	Median relative offset in timing of growth rate change [%]
normal	10-20	10-40	middle third	10-100	12-17	66.3	10.5
high DCF	10-20	10-40	middle third	10-100	6-23	34.9	19.9
fast growth	10-20	10-40	middle third	50-500	12-17	29.1	17.2

The detection rate of growth rate changes increases with more radiocarbon measurements (Fig. 2). This is valid for all three experiments, but at different levels. While for the 'normal' experiment about 2/3 of the realizations detected a growth rate change, the success rate of the other two experiments is only about 1/3 (compare Tab. 1). The success rate of the detection for the 'high DCF' experiment is lower as a result of the large reservoir effect variability, which is responsible for significant noise on the radiocarbon decay trend that masks any growth rate changes. This is especially true for stalagmites covering only a short period of time.

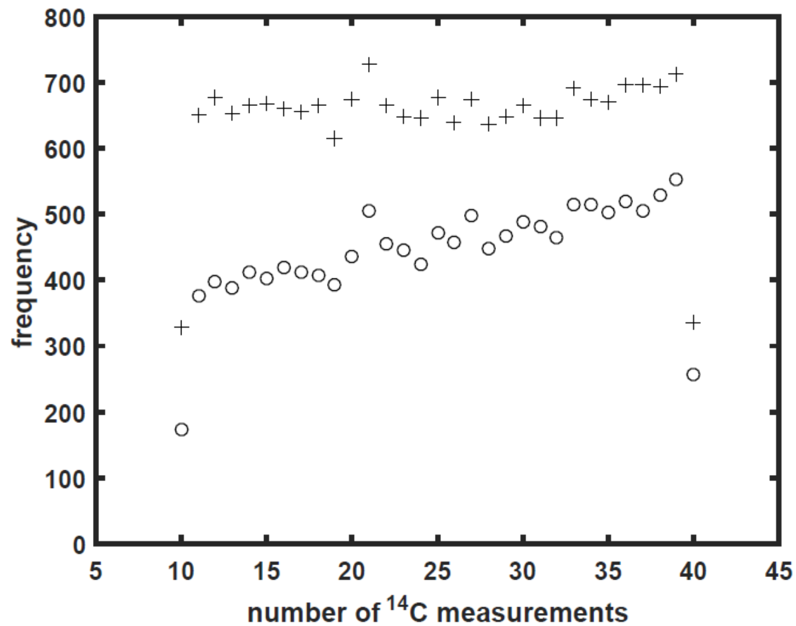

Fig. 2: *Frequency of randomly determined number of radiocarbon measurements (crosses) is evenly distributed for the 'normal' experiment. The open circles represent the number of artificially produced data sets with detected growth rate changes for the same experiment. Note the increase in detected growth rate changes with increasing number of radiocarbon measurements per sample.*

The reason for the low detection rate in the 'fast growth' experiment is related to the short time period covered by the artificially constructed stalagmite data sets. Short growth periods do not allow for enough radiocarbon decay to occur for a good fit. Although the reservoir effect variations are also kept small for this experiment, the signal (radiocarbon decay) to noise (reservoir effect variations) ratio remains too high to enable our approach to detect growth rate changes. This effect is well visible when comparing the relative detection rate over the growth duration of the stalagmite (Fig. 3). For stalagmites covering only 500 years the detection rate of a growth rate change is very low, but increases rapidly when stalagmites grow over longer time periods. For stalagmites growing over a period of more than 1500 years the detection rate reaches ~80% for the 'fast growth' experiment. For the 'normal' and 'high DCF' experiments the detection rate also strongly increases with growth duration (Fig. 3).

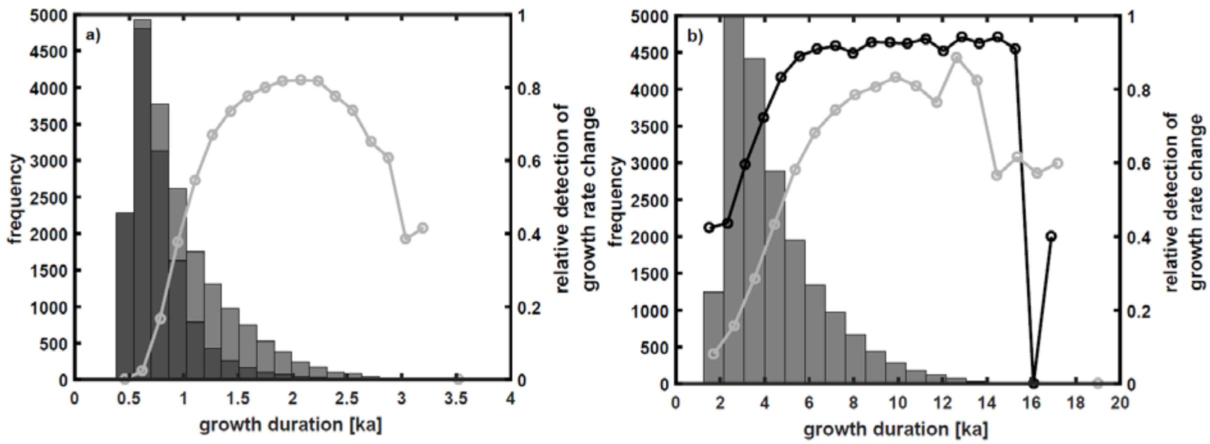

Fig. 3: *Frequency distribution and the relative detection of growth rate changes over the growth period length of the artificially constructed stalagmite age-depth models. a) Frequency distribution for all realisations of the 'fast growth' experiment (light grey bars) are shown as well as for those realisations with no detection (dark grey bars). Grey circles show the detection rate of growth rate changes. b) Frequency distribution for all realizations of the 'normal' experiment (for the 'high DCF' experiment the distribution looks similar) and its relative detection rate of the growth rate change (black circles). Grey circles represent the detection rate for the 'high DCF' experiment.*

The detection rate of growth rate changes varies strongly and appears to decrease for longer data sets (> 2.5 ka for the 'fast growth' experiment, >13 ka for both other experiments). However, this is an artefact due to the low number of long growing synthetic datasets constructed here, as the detection rate for data sets with a long growth period should remain high. This is indicated by the low relative proportion of growth rate change detection for long growing stalagmites of the 'fast growth' experiment (Fig. 3; growth period between present day and 2.5 to ~3.6 ka) and the high detection rate for the 'normal' experiment for the same growth period.

Interestingly, the relative detection rate for all three experiments is not the same for similar growth durations. For the 'high DCF' experiment this is not a surprise due to the strong noise introduced by the large reservoir effect variability. It is somewhat surprising however for the experiments which only differ by their growth rates. For example, the detection rate of a growth rate change for a typical 2 ka old stalagmite within the 'fast growth' data set is about 80% while for the 'normal' experiment a successful detection is only obtained for only about 40% of all synthetic data sets. This difference is caused by the different absolute change in growth rate changes possible for each data set, as the program more easily detects larger absolute variations in growth rate. For the 'normal' experiments the growth rate was prescribed to be within a range of 10 to 100 µm, and thus the absolute growth rate change is much smaller (i.e., maximum 90 µm) than what is possible for a 'fast growth' stalagmite, where the growth range was prescribed between 50 to 500 µm (maximum change 450 µm). Larger absolute variations in growth rate can be much more easily detected by our program. This can be also expressed in a different way: the longer the period where speleothems grow with the same growth rate, the more likely it is to detect also small absolute changes in growth rate. With more radiocarbon measurements available it becomes easier to detect smaller absolute growth rate changes as well (Fig. 4). A similar behaviour is detected for all three types of experiment.

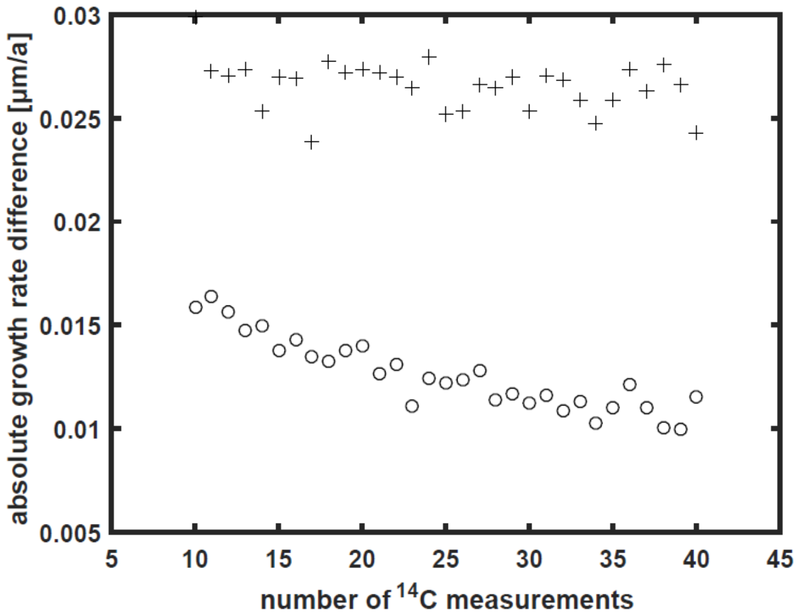

Fig. 4: *The average for the absolute difference of growth rates for the successful detection of growth rate changes for the realizations of the 'normal' experiment is ~0.026 µm/a (crosses) for any number of radiocarbon measurements. The absolute difference of growth rates with an unsuccessful detection of growth rate changes decreases with the number of radiocarbon measurements (circles).*

An additional positive effect of a larger number of radiocarbon measurements for a given (synthetically produced) stalagmite data set is the smaller average absolute age deviation between the modelled and artificially produced age-depth relationships (Fig. 5). For the 'normal' experiment the average absolute age deviation for realizations with successful growth rate change detection is reduced from ~120 to ~100 a when the number of radiocarbon measurements is increased from 10 to 40. If the growth rate change was not detected, the average deviation between the modelled and artificially produced age-depth relationships is even smaller. In this case, the average absolute age offset is reduced from about 110 a (with 10 samples) to ~80 a (with 40 samples; Fig. 5). This proves very nicely that for those cases where the growth rate change has not been detected (e.g., due to low absolute growth rate differences or short growth duration), the average absolute age offset between modelled and true age-depth relationship is already relatively small. In other words, in cases where the average absolute growth offset for the modelled linear age-depth relationship is large, a growth rate change is usually detected. Then the recalculation of the age model with two phases of different growth rates minimises the age offset. This shows that even if growth rate changes are not detected, the obtained age-depth relationship is reliable.

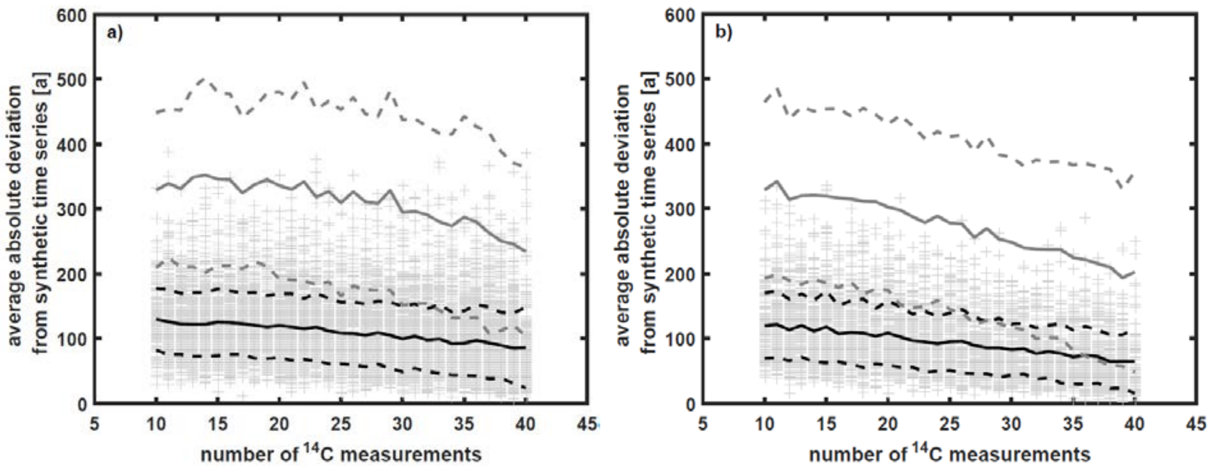

Fig. 5: *Absolute value of the average age offset between age-depth modelling results and their actual synthetic age-depth relationship for the 'normal' experiment (Tab. 1). a) Results for cases where the growth rate change was detected; b) results for cases where the growth rate change detection failed. Crosses represent the results of individual realizations, while solid and dashed black lines represent the average and standard deviation of the individual realizations for a given number of radiocarbon measurements. Grey solid and dashed lines represent the average absolute age offset and standard deviation when the range in DCF is between 23 and 6% ('high DCF' experiment, Tab. 1). Individual results for this scenario are not shown.*

The age offset between modelled and artificially constructed age-depth relationship becomes much larger if the radiocarbon reservoir effect strongly varies (Fig. 5). For the successful detection of a growth rate change in the 'high DCF' experiment the average age offset between modelled and true age-depth relationship is reduced from ~350 to 250 a when the number of radiocarbon measurements is increased from 10 to 40. If the growth rate change is not detected, the age offset is reduced from ~330 to 200 a with increasing number of radiocarbon measurements. Again, the age offset for the unsuccessful detection of growth rate changes is smaller than for the successful growth rate change detections.

This large average age offset between modelled and true age-depth relationship for the 'high DCF' experiments should not concern potential users. A data compilation of available reservoir effect variations of published records indicates that usually the reservoir effect variations are in the range of +/- 2.5 % (Hua et al., 2017), similar as prescribed for the 'normal' experiment in this study. The large DCF variation of the 'high DCF' experiment (+/- 8.5 %) are only chosen to better exemplify the influence of the strength of reservoir effect variations and were only observed in extreme locations so far (e.g., Genty et al., 2001; Bajo et al., 2017).

Our method reliably reproduces the timing of growth rate changes in synthetically produced stalagmite datasets (Fig. 6a). For all synthetic datasets produced, the relative age offset between prescribed and modelled timing of the growth rate change is very small and nearly independent of the amount of radiocarbon measurements for more than ~20 measurements.

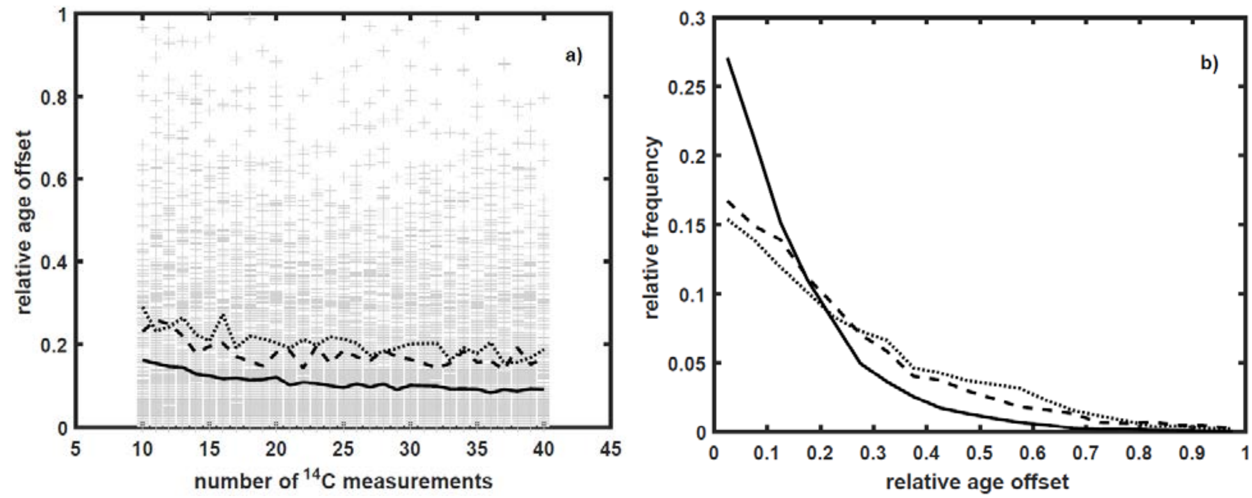

Fig. 6: a) The relative age offset of the modelled vs prescribed timing of the growth rate changes over the number of radiocarbon measurements. Grey crosses represent the individual offset of the modelled vs prescribed timing of the growth rate change for the 'normal' experiment. The solid line indicates the median offset for a given amount of radiocarbon measurements in this experiment. The median values for the 'high DCF' and 'fast growth' experiment are represented by the dotted and dashed lines. b) Relative frequency of the relative age offsets for the timing of the growth rate change. Line coding is as in a).

For the 'normal' experiment, the median relative age offset for the timing of the growth rate change is ~10.5 %. The offset is slightly larger for the 'high DCF' (19.9 %) and the 'fast growth' (17.2 %) experiments, but again not strongly affected by the number of measurements, especially when >20 samples are available. Approximately 75 % of all successfully detected growth rate changes find the position within a 20 % range for the 'normal' experiment. Only about 0.3 % of all successfully detected growth rate changes have an offset for the timing of the age offset of larger than 100 %.

Similar observations can be drawn when comparing the prescribed and modelled growth rates before and after the timing of growth rate change (Fig. 7). Both growth rates, before and after the growth rate change are well reproduced by star, in most cases with only a small offset. About 90 % (85%) of all iterations have a relative growth rate offset not larger than 20 % for growth rate before (after) the change in the 'normal' experiment. The relative growth rate offsets for the other two experiments are larger. More than 55 % of all iterations for both other experiments obtain offsets smaller than 20 % for growth rates before and after the growth rate change.

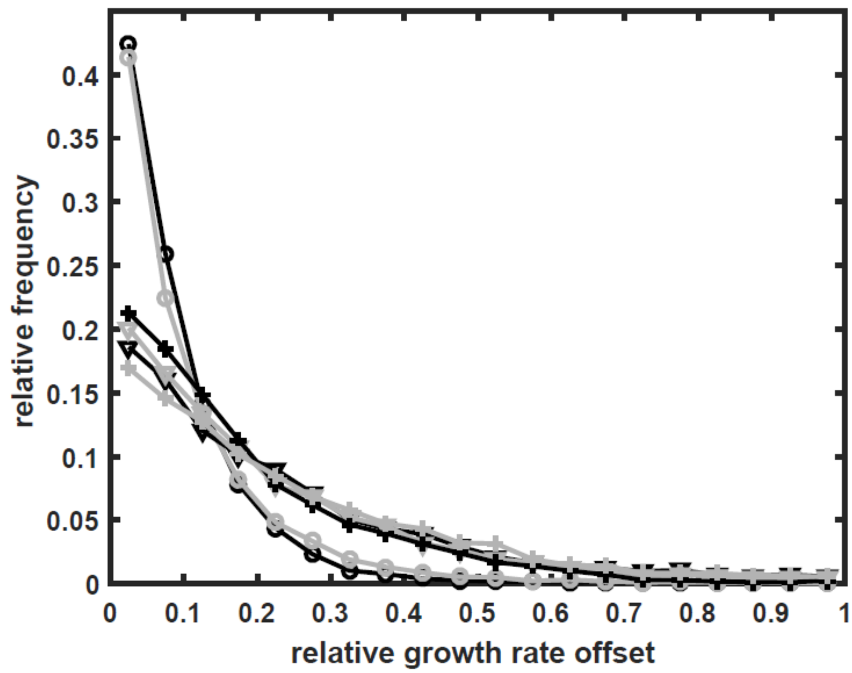

Fig. 7: Relative growth rate offsets for all three types of experiments for the period before (grey) and after (black) the growth rate change. Circles – 'normal', plus signs – 'fast growth' and triangles – 'high DCF' experiment.

4. Application to existing speleothem 14C data

The application of our method to 'real' stalagmites is still difficult, due to the paucity of published datasets that provide a precise U-Th based chronology and radiocarbon measurements spanning longer than ~ 500 years. Here, we focus on four stalagmites, starting with a specimen that fulfils all requirements for the use of our age-depth modelling approach (Sec. 4.1). It is easier to learn about the limits of this approach with examples where the age-depth modelling is not entirely successful, thus we successively choose specimen with an increased degree of complexity: (1) trends in $\delta^{13}C$ or Mg/Ca which hint to a violation of the stationarity assumption in the reservoir effect (Sec. 4.2) and (2) multiple changes in growth rate (Sec. 4.3). Finally, we apply the method even to a stalagmite with secondary long-term reservoir effect variations, which can be approximated by a polynomial of fourth order (Sec.4.4). This approach illustrates the effects of trends in the reservoir effect on the calculation of age-depth models.

4.1 Stalagmite HS4 – Heshang cave

As in Lechleitner et al. (2016b), we first focus on the precisely U-Th dated stalagmite HS4 from Heshang Cave, China, which grew during the Holocene and has more than 80 radiocarbon measurements (Noronha et al., 2014). We compare the original age-depth model (Hu et al., 2008) with the age-depth relationship published with the first version of *star* (Lechleitner et al., 2016) and with the model output for the recent version of our approach (Fig. 8a). In addition, we show the DCF as derived for the U-Th based age-depth model and the results for the recent approach (Fig. 8b) as well as Mg/Ca and $\delta^{13}C$ values (Fig. 8c; Noronha et al., 2014, Hu et al., 2008).

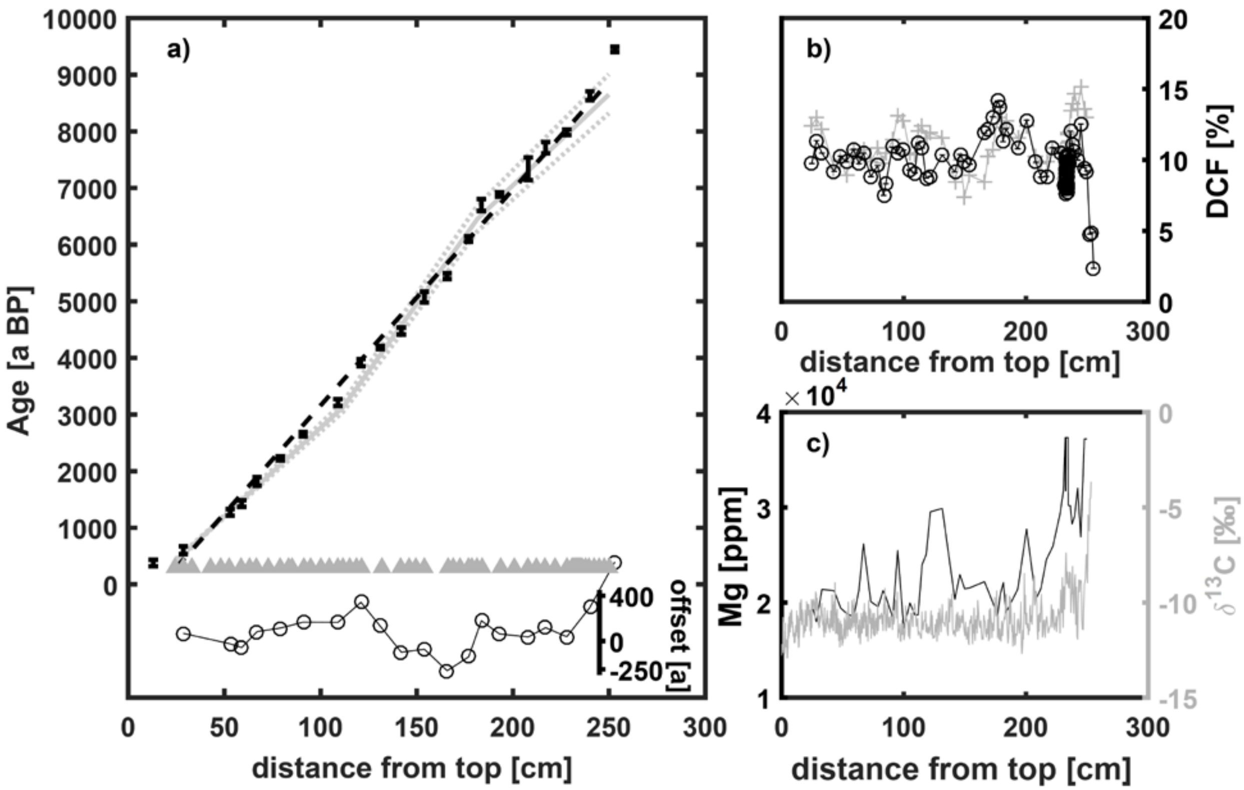

Fig. 8: *a) Comparison of age-depth relationships as provided by U-Th dating (black signs, with error bars) and from radiocarbon measurements using the first version of star (dashed black line; Lechleitner et al., 2016) and the version presented in this study (solid grey line, plus error envelope – dotted grey lines). The anchor point for both versions was a U-Th age of 0.985 ka at 43 cm depth from top. Triangles represent the depths of radiocarbon measurements. Open circles show the deviation between the U-Th ages and result of the present star-version. b) DCF as calculated based on the U-Th chronology in Noronha et al. (2014, black) and as resulted from the radiocarbon age-depth modelling (this study, grey). c) The Mg/Ca and* $\delta^{13}C$ *data sets show no long-term trend, corroborating the absence of secular trends in DCF.*

The ancillary $\delta^{13}C$ values are not affected by consistent and long-term trends, while Mg/Ca only shows a weak linear trend within the oldest fifth of the record (Fig. 8c). Thus, a warning is given by *star* that the stationarity of the reservoir effect might be compromised. However, in this case, the high precision U-Th chronology allows calculation of the true reservoir effect (Noronha et al. 2014), which indeed proves to be stationary but with a noisy structure (Fig. 8b). This allows us to apply our approach and highlights the fact that even if there are trends in the ancillary proxies, this does not necessarily translate to non-stationarity in the reservoir effect, as these relationships are not perfect. Thus, a trends in the ancillary proxies does not preclude the use of *star*, but rather the user needs to assess the likelihood of a relationship between ancillary proxies and DCF. The DCF varies between ~7 and 14 % (+/-3.5 % around the mean value) and thus is comparable with the 'normal' dataset of synthetic records, discussed in Sec. 3.2. With its long growth duration (~9 ka) and fast growth rate (average 270µm/a), this specimen is perfectly suited to apply *star*. Indeed, the model results compare well to the U-Th ages, especially when applying the updated model version presented here, as the true growth history is reproduced much more closely than in the previous model version (Fig. 8a). This is a result of the newly included function to detect and implement growth rate changes. The excellent match between calculated and modelled DCF values emphasizes how well star can capture the real growth history of a stalagmite (Fig. 8b).

4.2 Stalagmite CC26 - Corchia cave

A recently published dataset from stalagmite CC26 from Corchia Cave, Italy, includes a precise U-Th based chronology as well as Mg/Ca, $\delta^{13}C$, and radiocarbon data (Regattieri et al., 2014; Bajo et al., 2017). While no long term trend in Mg/Ca is detected, $\delta^{13}C$ values gradually decrease from +3 to -2‰ (Fig 9c). It is also worth noting that the $\delta^{13}C$ values in this stalagmite are exceptionally high compared to other stalagmites, an indication of the unusual depositional conditions in this cave (Bajo et al., 2017). The trend in $\delta^{13}C$ prompts a warning about possibly compromised age-depth modelling in the software. This is indeed the case, as the U-Th-derived DCF is affected by a long-term trend, synchronous with the $\delta^{13}C$ trend (Fig. 9b; Bajo et al., 2017). This threatens the stationarity assumption of our approach. Here, we investigate the impact of this trend in DCF on the resulting radiocarbon based chronology (Fig. 9a).

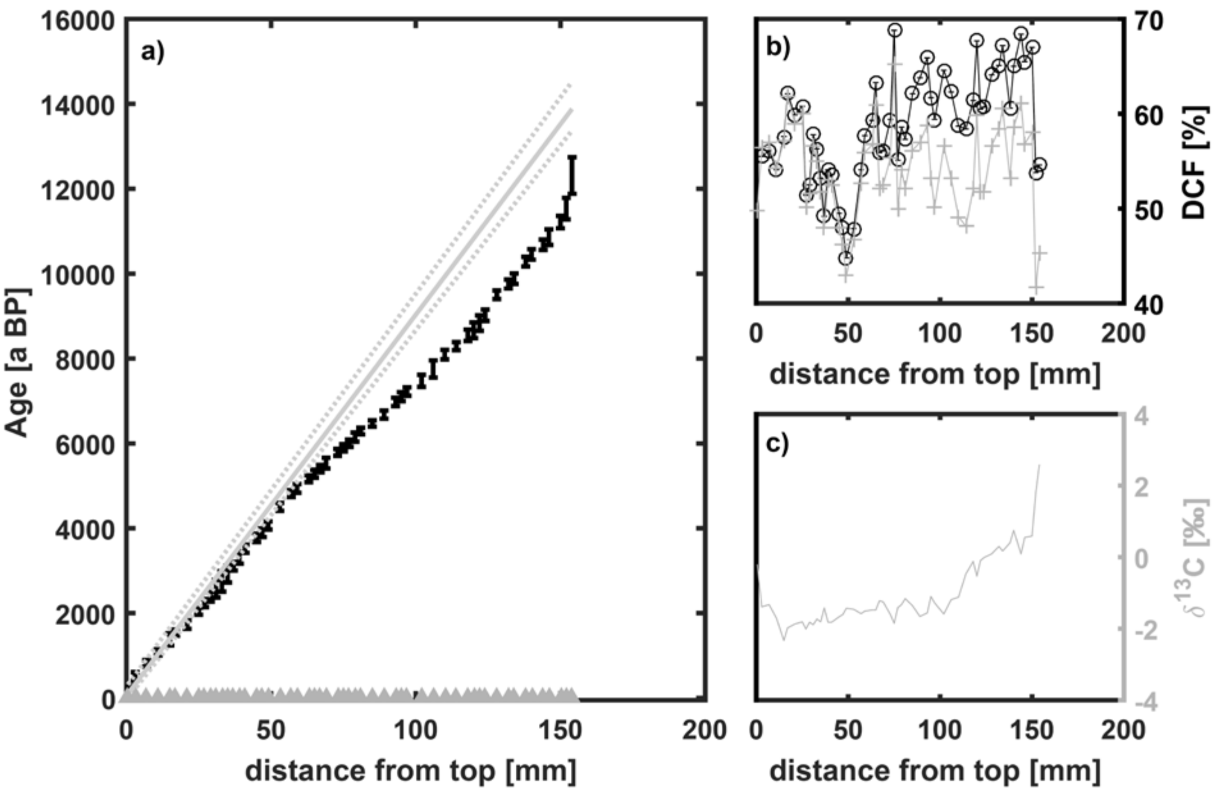

Fig. 9: *a) True, U-Th based age depth model of stalagmite CC26 (black, Bajo et al. 2017) and the result of the radiocarbon based age-depth model (grey) with uncertainties (grey shaded area). The anchor point is 102 years at 0.5 mm from top. Black signs represent U-Th dates with their errors. Grey triangles at the bottom indicate the depths of radiocarbon measurements. b) Reservoir effect variations over depth with respect to the U-Th based age depth model (black) and after the radiocarbon based one (grey). c) Carbon isotope composition over depth of stalagmite CC26.*

The modelled age-depth relationship follows the U-Th based chronology faithfully in the youngest part of the record (~ 6 ka to present, Fig. 9a). However, the two age models increasingly diverge in the earlier part of the record, as the true DCF steadily increases and moves away from stationarity (Fig. 9b). The radiocarbon based age-depth modelling approach is not able to detect the growth rate change at ~60-70 cm depth. As a result, *star* interprets the DCF trend as a considerably older growth history (~1500 a older at the bottom; Fig. 9a). This example illustrates well how providing additional ancillary proxies that reflect processes affecting the DCF can be crucial for the final evaluation of the age-depth model. On a positive note, we show that the model agrees very well with the U-Th chronology for the younger part of CC26, where the stationarity criterion is met, and that the very high and variable DCF (between 44 and 64 %) does not preclude a successful application of this approach.

In addition, we tested how the input of less radiocarbon data affects the age-depth modelling result. The final result is nearly unchanged even removing one third or half of the radiocarbon measurements. The influence of a few, single measurement points was also tested by removing them individually. As expected, the final result of the age-depth model does not change if the values we tested lie in the centre of the stalagmite. However, if radiocarbon measurements are removed at the stalagmite top, the model result changes substantially, as *star* finds two points where growth rate changes could have occurred. Interestingly, under this conditions the model performs slightly better for the older part (>6 ka) than the youngest interval. Thus the top and bottom of a target stalagmite require denser sampling, while within the stalagmite sampling density does not be as high. This is useful especially with respect to the considerable cost of radiocarbon measurements.

4.3 Stalagmite MC3, Moaning Cave

Next, we apply our model to flowstone MC3 from Moaning cave, Nevada (Oster et al., 2010), where the anchor point is located in the flowstone section with a long-term trend in DCF (derived from the U-Th chronology; Fig. 10b). Previous studies have highlighted the complicated influences on $\delta^{13}C$ and Mg/Ca in this cave system, which are believed to reflect not only humidity changes but also shifts in the drip centre of the flowstone (Oster et al., 2009). While $\delta^{13}C$ data in stalagmite CC26 from Corchia cave reflected the presence of a trend in DCF, the stable isotope data available for MC3 does not show any long-term trend but large fluctuations (Fig. 10c). In contrast, Mg shows a long term trend (Fig. 10c), which illustrates the advantage of having both proxies available.

MC3 has 12 U-Th dated depths that reveal its complicated growth history. Three phases with different growth rates can be derived. A fast growth on the top (between ~10 and 20 mm), slow growth between ~20 and 25 mm culminating in extremely slow growth at ~23 mm, and higher growth rate again below ~25 mm. Our age-depth modelling approach reproduces the growth history of the top ~23 mm extremely well but mostly fails to reproduce the U-Th based ages within the oldest part (> ~23 mm), where only the very upper age error of our approach overlaps with the U-Th results. The reason for this discrepancy is in the change in the reservoir effect, as seen from the DCF derived from the U-Th based chronology. As *star* assumes that there is no change in the reservoir effect for the time of the absence of $CaCO_3$ precipitation, the offset in the age can be well explained by the reservoir effect change.

However, the trend in Mg before the growth stop is already an indication of systematic carbonate dissolution changes. This is encouraging, as with a better understanding of C systematics within the soil-karst-cave environment this issue could be potentially resolved in future versions of *star*. In the present model version, the result evaluation critically depends on informed decisions by the user, based on knowledge of the local conditions and speleothem morphology.

Our approach also suggests the presence of a hiatus in the extremely slow growth section (~23 mm) (Fig. 10a). However, we want to emphasize that this phase of slow growth is understood not to reflect a deterioration in the local hydrologic conditions, but rather depicts changes in the drip centre and water flow downwards the flowstone. Thus, no $CaCO_3$ was deposited at the location of the flow stone core, which mimics a growth hiatus (Oster et al., 2009).

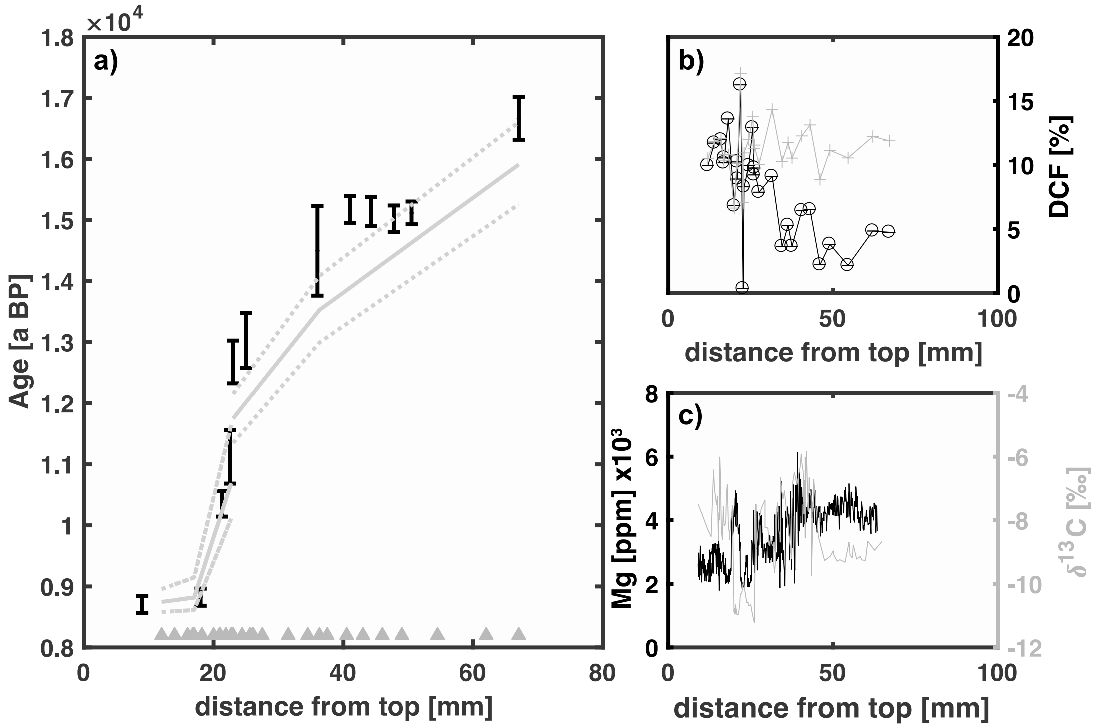

Fig. 10: *a) U-Th based age determinations of stalagmite MC3 (black, Oster et al. 2009; 2010; 2015) and the result of the radiocarbon based age-depth model (solid grey line) with uncertainties (dotted grey lines). Anchor point was 8.7 ka at 9 mm distance from top of the stalagmite. Grey triangles at the bottom represent the depths of radiocarbon measurements. b) Reservoir effect variations over depth with respect to the U-Th based age-depth model (black) and after the radiocarbon based one (grey). c)* δ^{13}C *(grey) and Mg (black) over depth of stalagmite MC3.*

4.4 Stalagmite YOK-I, Yok Balum Cave

As a last example, we test *star* on a precisely dated speleothem from Belize (YOK-I, Yok Balum Cave; Lechleitner et al., 2016, Kennett et al., 2012). Stable C isotope values (Fig. 10c) and the reservoir effect (Fig. 11b) do not show long-term linear trends (Fig. 11c). However, the reservoir effect does show secular variations (Fig. 11b), which might be approximated by a polynomial of fourth order. The model interprets these variations in the reservoir effect as growth rate variations, resulting in a failed reconstruction of the chronology (Fig. 11a). Otherwise, star would approximate the U-Th chronology well for its linear age-depth result (i.e., before it is searching for growth rate changes).

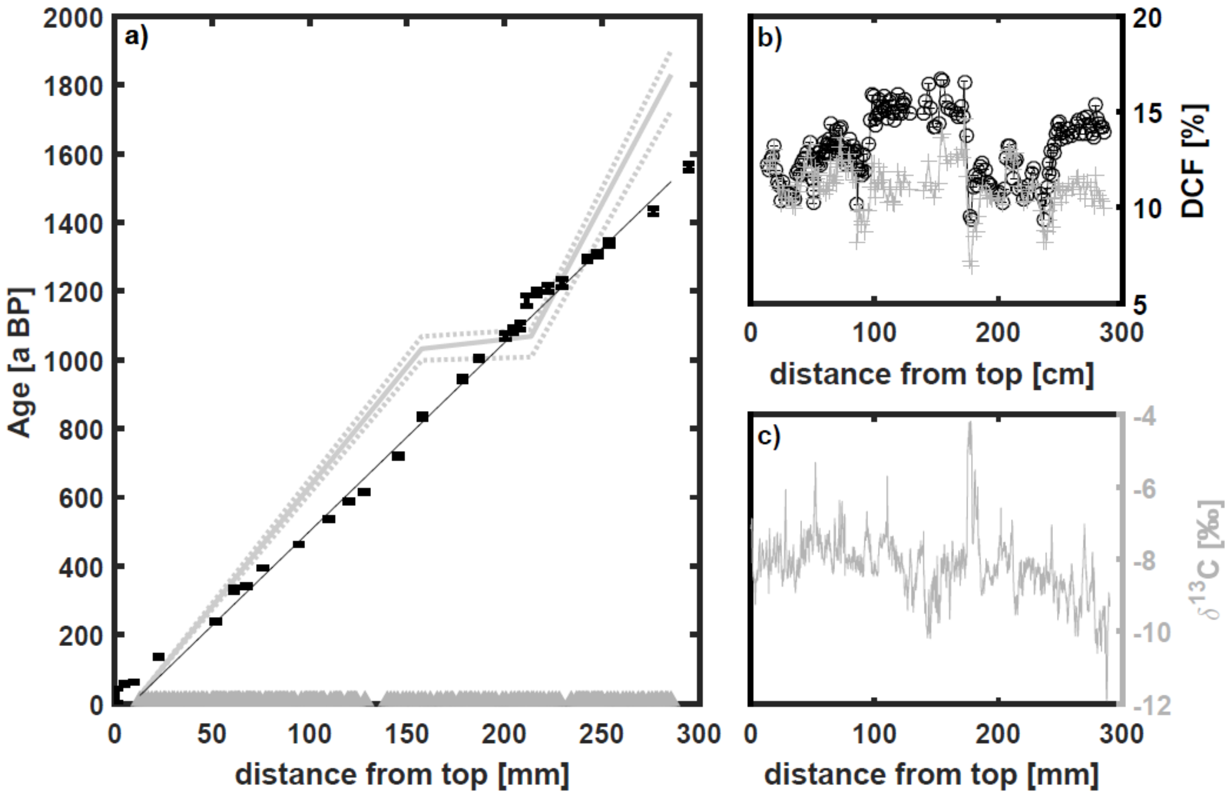

Fig. 11: *a) U-Th based age determinations of stalagmite YOK-I (black, Kennett et al., 2012) and the result of the radiocarbon based age-depth model (solid grey line) with uncertainties (dotted grey lines). Anchor point was 23 years at 12.8 mm distance from top of the stalagmite, the last radiocarbon measurement before the onset of the radiocarbon bomb pulse. The thin black line represents the linear age-depth model found by star. Grey triangles at the bottom represent the depths of radiocarbon measurements. b) Reservoir effect variations over depth with respect to the U-Th based age-depth model (black, Lechleitner et al., 2016a) and after the radiocarbon based model (grey). c)* δ^{13}C *(grey) over depth of stalagmite YOK-I.*

As the program module for the recognition of growth rate changes uses polynomial remnants of reservoir effect variations, the secondary natural DCF variations for YOK-I are interpreted as growth rate changes. The positions of the growth rate changes are close to the position with the maximum and minimum DCF (determined from the U-Th chronology) at ~140 and 210 mm distance from top. This example illustrates the complexity of our newly included functions with respect to the requirements of the stationarity of the radiocarbon reservoir effects. Structured DCF variations can now disturb an otherwise reliable age-depth model. However, only this study by Lechleitner et al. (2016) revealed that those long-term structures can be implemented in stalagmite radiocarbon reservoir effects. Reservoir effect structures, acting on a shorter period of time, will not have any effect on the resulting age-depth model.

5. Conclusion

We present an improved age-depth modelling approach based on reservoir effect loaded radiocarbon measurements. The program is now able to detect growth stops, can handle major growth rate variations and is able to warn the user if the radiocarbon measurements are likely to be subject to trends in the reservoir effect. The latter point, however, might be regarded as not conclusive as it represents a trend evaluation after recent knowledge about radiocarbon reservoir effect variability. More work on C transfer dynamics from the atmosphere to the cave is needed to increase confidence in this new function.

Growth stops can be detected, but need justification by the user. As fast reservoir effect variations can occur within short periods, an automated mechanism is not applicable. The user should also confirm the radiocarbon evidence by additional information, e.g., optically visible layers or evidence from geochemical data. The most important improvement is the detection of phases with different growth rates. For the present model version, we show that major growth rate variations are more likely detected. The larger the difference between two consecutive growth rates and the more radiocarbon measurements are available as well as the more time between phases of different growth rates elapsed the more likely it is to find phases with different growth rates. The precision of the age-depth models depends also strongly on the length of the growth period and on the variability of the reservoir effect, as large scatter in the DCF impede the fitting procedure, or at least result in larger error estimates of the mean growth rate fit.

In summary, this new version of our radiocarbon based age-depth modelling approach can be compared with age models derived by U-Th dated stalagmites in the early 2000s, when similar piece-wise constant growth, linear age-depth models were mostly used to describe the growth history of stalagmites. Realistically, any further improvement of the present-day status of our software would require an enormous addition of knowledge of C transfer dynamics in karst environments. Such insights would allow us to implement better options for the evaluation of trends in the radiocarbon reservoir effect, and to account for them. Even with the recent improvements on *star*, U-Th dating remains the best option for stalagmite dating when possible, as this method will provide a much better age control. However, our software provides an option to reliably model the age-depth relationship using radiocarbon for stalagmites that cannot be dated using U-Th.

Finally, we want to mention that *star* is also well applicable to reservoir effect loaded radiocarbon measurements from other archives, such as ground water aquifers, lake sediments or travertines as long as the requirements of our approach can be regarded as (nearly) fulfilled.

Acknowledgements

JF is supported by DFG grants FO 809/2-1 and FO 809/4-1. FL acknowledges funding by the Swiss National Science Foundation grant P2EZP2_172213. We are grateful to Jessica Oster and an anonymous reviewer for their thorough review and constructive criticism, which lead to important improvements of the manuscript.

Code availability

The code is available on github: https://github.com/jensfohlmeister/star.git.

References

Bajo, P., Borsato, A., Drysdale, R., Hua, Q., Frisia, S., Zanchetta, G., Hellstrom, J., Woodhead, J., 2017. Stalagmite carbon isotopes and dead carbon proportion (DCP) in a near-closed-system situation: An interplay between sulphuric and carbonic acid dissolution. Geochimica et Cosmochimica Acta 210, 208-227.

Benavente, J., Vadillo, I., Carrasco, F., Soler, A., Linan, C., Moral, F., 2010. Air carbon dioxide contents in the vadose zone of a Mediterranean karst. Vadose Zone Journal 9, 126-136.

Bergel, S. J., Carlson, P. E., Larson, T. E., Wood, C. T., Johnson, K. R., Banner, J. L., Breecker, D. O., 2017. Constraining the subsoil carbon source to cave-air CO2 and speleothem calcite in central Texas. Geochimica et Cosmochimica Acta, 217, 112-127.

Deininger, M., Fohlmeister, J., Scholz, D., Mangini, A., 2012. The influence of evaporation effects on the carbon and oxygen isotope composition of speleothems - a model approach. Geochimica et Cosmochimica Acta 96, 57-79.

Dreybrodt, W., 2008. Evolution of isotopic composition of carbon and oxygen in a calcite precipitating H2O-CO2-CaCO3 solution and the related isotopic composition of calcite in stalagmites. Geochimica and Cosmochimica Acta 72, 4712-4724.

Dreybrodt, W., Scholz, D., 2011. Climatic dependence of stable carbon and oxygen isotope signals recorded in speleothems: From soil water to speleothem calcite. Geochimica et Cosmochimica Acta 75, 734-752.

Fairchild, I. J., Baker, A., 2012. Speleothem science: From process to past environments. Wiley-Blackwell.

Fairchild, I. J., Treble, P. C., 2009. Trace elements in speleothems as recorders of environmental change. Quaternary Science Reviews 28, 449-468.

Fohlmeister, J., Arps, J., Spötl, D., Schröder-Ritzrau, A., Plessen, B., Günter, C., Frank, N., Trüssel, M., 2018. Carbon and oxygen isotope fractionation in the water-calcite-aragonite system. Geochimica et Cosmochimica Acta, 235, 127-139.

Fohlmeister, J., Plessen, B., Dudashvili, A. S., Tjallingii, R., Wolff, C., Gafurov, A., Cheng, H., 2017. Winter precipitation changes during the Medieval Climate Anomaly and the Little Ice Age in arid Central Asia. Quaternary Science Reviews 178, 24-36.

Fohlmeister, J., Scholz, D., Kromer, B., Mangini, A., 2011. Modelling carbon isotopes of carbonates in cave drip water. Geochimica et Cosmochimica Acta 75, 5219-5228.

Fohlmeister, J., Schröder-Ritzrau, A., Spötl, C., Frisia, S., Miorandi, R., Kromer, B., Mangini, A., 2010. The influences of hydrology on the radiogenic and stable carbon isotope composition of cave drip water, Grotta di Ernesto (Italy). Radiocarbon 52, 1529-1544.

Genty, D., Baker, A., Massault, M., Proctor, C., Gilmour, M., Pons-Branchu, E., Hamelin, B., 2001. Dead carbon in stalagmites: carbonate bedrock paleodissolution vs. ageing of soil organic matter. Implications for ^{13}C variations in speleothems. Geochimica et Cosmochimica Acta, 65, 3443-3457.

Griffiths, M. L., Fohlmeister, J., Drysdale, R. N., Hua, Q., Johnson, K. R., Hellstrom, J. C., Gagan, M. K., Zhao, J.-x., 2012. Hydrological control on the dead-carbon content of a Holocene tropical speleothem. Quaternary Geochronology 14, 81-93.

Hua, Q., Cook, D., Fohlmeister, J., Penny, D., Bishop, P., Buckman, S., 2017. Radiocarbon Dating of a Speleothem Record of Paleoclimate for Angkor, Cambodia. Radiocarbon 59, 1873-1890.

Hua, Q., McDonald, J., Redwood, D., Drysdale, R., Lee, S., Fallon, S., Hellstrom, J., 2012. Robust chronological reconstruction for young speleothems using radiocarbon. Quaternary Geochronology 14, 67-80.

Kennett, D. J., Breitenbach, S. F., Aquino, V. V., Asmerom, Y., Awe, J., Baldini, J.U.L., Bartlein, P., Culleton, B.J., Ebert, C., Jazwa, C., Macri, M.J., Marwan, N., Polyak., V., Prufer, K.M., Ridley, H.E., Sodemann, H, Winterhalder., B., Haug., G.H., 2012, Development and disintegration of Maya political systems in response to climate change. Science, 338, 788-791.

Lechleitner, F. A., Baldini, J. U. L., Breitenbach, S. F. M., Fohlmeister, J., McIntyre, C., Goswami, B., Jamieson, R. A., van der Voort, T. S., Prufer, K., Marwan, N., Culleton, B. J., Kennett, D. J., Asmerom, Y., Polyak, V., Eglinton, T. I., 2016a. Hydrological and climatological controls on radiocarbon concentrations in a tropical stalagmite. Geochimica et Cosmochimica Acta 194, 233-252.

Lechleitner, F. A., Fohlmeister, J., McIntyre, C., Baldini, L., Jamieson, R. A., Hercman, H., Gasiorowski, M., Pawlak, J., Stefaniak, K., Socha, P., Eglinton, T. I., Baldini, J. U. L., 2016b. A novel approach for reconstruction of accurate radiocarbon-based chronologies for speleothems. Quaternary Geochronology 35, 54-66.

Minami, M., Kato, T., Horikawa, K., Nakamura, T., 2015. Seasonal variations of ^{14}C and $\delta^{13}C$ for cave drip waters in Ryugashi Cave, Shizuoka Prefecture, central Japan. Nuclear Instruments and Methods in Physics Research Section B: Beam Interactions with Materials and Atoms 362, 202-209.

Noronha, A. L., Johnson, K. R., Hu, C. Y., Ruan, J.-Y., Southon, J., Ferguson, J. E., 2014. Assessing influences on speleothem dead carbon variability over the Holocene: implications for speleothem-based radiocarbon calibration. Earth and Planetary Science Letters 394, 20-29.

Noronha, A. L., Johnson, K. R., Southon, J. R., Hu, C., Ruan, J., McCabe- Glynn, S., 2015. Radiocarbon evidence for decomposition of aged organic matter in the vadose zone as the main source of speleothem carbon. Quaternary Science Reviews 127, 37-47

Oster, J. L., Montanez, I. P., Guilderson, T. P., Sharp, W. D., Banner, J. L., 2010. Modeling speleothem $\delta^{13}C$ variability in a central Sierra Nevada cave using ^{14}C and $^{87}Sr/^{86}Sr$. Geochimica et Cosmochimica Acta 74, 5228-5242.

Oster, J. L., Montanez, I. P., Santare, L. R., Sharp, W. D., Wong, C., Cooper, K. M., 2015. Stalagmite records of hydroclimate in central California during termination 1. Quaternary Science Reviews 127, 199-214.

Oster, J. L., Montanez, I. P., Sharp, W. D., Cooper, K. M., 2009. Late Pleistocene California droughts during deglaciation and Arctic warming. Earth and Planetary Science Letters, 288, 434-443.

Reimer, P. J., Bard, E., Bayliss, A., Beck, J. W., et al., 2013. IntCal13 and Marine13 radiocarbon age calibration curves 0-50,000 years cal BP. Radiocarbon 55, 1869-1887.

Rudzka, D., McDermott, F., Baldini, L. M., Fleitmann, D., Moreno, A., Stoll, H., 2011, The coupled δ13C-radiocarbon systematics of three Late Glacial/early Holocene speleothems; insights into soil and cave processes at climatic transitions. Geochimica et Cosmochimica Acta, 75, 4321-4339.

Rudzka, D., McDermott, F., Suric, M., 2012. A late Holocene climate record in stalagmites from Modric Cave (Croatia). Journal of Quaternary Science 27, 585-596.

Scholz, D., Frisia, S., Borsato, A., Spötl, C., Fohlmeister, J., Mudelsee, M., Miorandi, R., Mangini, A., 2012. Holocene climate variability in North- Eastern Italy: Potential influence of the NAO and solar activity recorded by speleothem data. Climate of the Past 8, 1367-1383.

Scholz, D., Mühlinghaus, C., Mangini, A., 2009. Modelling $\delta^{13}C$ and $\delta^{18}O$ in the solution layer on stalagmite surfaces. Geochimica et Cosmochimica Acta 73, 2592-2602.

Sinclair, D. J., Banner, J. L., Taylor, F. W., P., J., Jenson, J., Mylroie, J., Goddard, E., Quinn, T., Jocson, J., Miklavic, B., 2012. Magnesium and strontium systematics in tropical speleothems from the Western Pacific. Chemical Geology 294, 1-17.

Zhang, H., Cai, Y., Tan, L., Qin, S., An, Z., 2014, Stable isotope composition alteration produced by the aragonite-to-calcite transformation in speleothems and implications for paleoclimate reconstructions. Sedimentary Geology 309, 1-14.